Role of particle network in concentrated mud suspensions

C. Ancey
Cemagref, Domaine Universitaire, 38402 Saint-Martin d'Hères, France

Keywords: rheophysics, constitutive equation, viscoplasticity, particle suspension

ABSTRACT: Most materials involved in debris flows are made up of solid particles in water, covering a large size range. When natural suspensions can be tested with the usual laboratory rheometers, they exhibit a wide range of bulk rheological properties (time-dependent effects, viscoplasticity, etc.) and flow effects (particle migration, shear localization). Such properties are difficult to understand and describe in the framework of continuum mechanics, in which they are most often expressed. A rheophysical approach is an alternative and fruitful way to describe the dynamics of geosuspensions. This paper reviews the main notions that are useful for understanding the rheological properties exhibited by natural mud suspensions. For concentrated suspensions, emphasis is given to the role played by a percolating network of coarse particles and the nature of contact between particles. Through a series of simple laboratory experiments, it is shown that a wide range of rheological behaviors can be observed by merely changing the particle size distribution.

1 INTRODUCTION

In engineering applications and zoning, it is of great interest to obtain accurate estimates of the main features of debris flows (volume, flow depth, impact pressure, etc.). This has motivated the development of computational tools specifically devoted to this purpose. Among the various approaches to computing debris-flow features, the fluid-mechanics approach has been extensively used to obtain a set of equations describing the motion of a debris flow from initiation to runout. Basically, these equations include mass and momentum balance equations together with a rheological (or constitutive) equation. Though there are different ways of expressing the equations of motion (local equations, depth-integrated equations, etc.), there is a wide consensus on their reliability and degree of approximation. In contrast, there is less consensus concerning rheological aspects: a large number of constitutive equations (Bingham, power-law fluid, Newtonian, etc.) have been proposed and used to describe debris flow motion but it still is unclear whether this diversity reflects the variety in the rheological properties of the materials involved in debris flows or merely a disagreement within

the scientific community on this point. In the debate around the determination of the rheological properties, a number of rheometrical experiments on debris flow samples have been performed to gain insight into their rheological behavior. To date, only partial evidence has been provided since, even with very large rheometers, only materials with a limited range of grain size can be tested and thus the question of how the full material behaves remains open. For instance, in the case of debris flow samples collected from deposits in the Alps, various rheometrical experiments have shown that the interstitial fluid behaves approximately as a viscoplastic (Herschel-Bulkley) fluid; extending this result to the material in its entirety has, however, been challenged.

The objective of this paper is to present the problem of the rheological properties of debris flow from a different perspective: if the constitutive equation reflects the material's mechanical behavior on a macroscopic scale, it can also be seen as a result of the interactions between particles and the interstitial fluid. The objective of this rheophysical approach is not only to determine the constitutive equation but also to explain and interpret its origin from physical considerations on the particle scale. I begin with suspensions of particles of approximately equal size, which is the simplest and more extensively studied type of suspension. Although Bagnold's pioneering work may be seen as the first attempt to deduce bulk behavior from local behavior in the area of particle suspensions, the theoretical foundations belong to Batchelor (1974). In the first part, I will outline the basics of this theoretical approach drawing from Batchelor's fundamental work. The key points in this presentation will be the notions of regime diagram, one- or two-phase flow on the macroscopic scale, and the percolating network of particles. It is fairly evident that equal-size particle suspensions cannot be seen as prototypical of natural materials; since the general case of polydisperse suspensions is overly complicated, a helpful approximation is to consider, in a first approximation, the case of bimodal suspensions. Applications of this rheophysical analysis to debris flows will be outlined in the conclusions.

2 AN OVERVIEW ON EQUAL-SIZE PARTICLE SUSPENSIONS

2.1 Local equations of motion

In the rheology of particle suspensions, the starting point in any rheophysical approach is to examine the behavior on a particle scale, then to infer the bulk rheological behavior by using an appropriate average process. In order to avoid overly general explanations, we assume that (i) the interstitial fluid is Newtonian, with viscosity μ and density ρ_f and (ii) the particles are rigid, spherical, and of equal size (radius a, density ρ_p). Fluid motion is described by the Navier-Stokes equations:

$$\frac{\partial \mathbf{u}_f}{\partial t} + \mathbf{u}_f \cdot \nabla \mathbf{u}_f = -\frac{1}{\rho_f}\nabla p + \frac{1}{\rho_f}\nabla \cdot \sigma_f \tag{1}$$

$$\nabla \cdot \mathbf{u}_f = 0 \tag{2}$$

where $\mathbf{u}_f$ is the fluid velocity, p is the generalized pressure (including the fluid pressure and gravity potential), and σ_f is the stress tensor (here $\sigma_f = 2\mu\mathbf{d}$ where $\mathbf{d}$ denotes the strain-rate tensor). The equation of motion for the particle can be written in the following Lagrangian

form:

$$\frac{d\mathbf{u}_p}{dt} = \mathbf{g} + \frac{1}{m_p}\mathbf{F}(\mathbf{u}_p, \mathbf{u}_f) \tag{3}$$

where $\mathbf{F}(\mathbf{u}_p, \mathbf{u}_f)$ is the force field resulting from the interaction between the fluid and the particle, m_p is the particle mass, and $\mathbf{u}_p$ the velocity of the mass center.

To obtain a more physical picture of the fluid/particle interplay, we will introduce dimensionless numbers and transform the equations above into dimensionless expressions. Let us introduce a velocity scale U for the fluid. The time scale for the fluid motion near the particle is then: a/U. The characteristic time for the particle is defined as a relaxation time, that is, the time needed for its velocity to vary substantially as a result of the fluid action. If F is the order of magnitude of the fluid-particle interaction, examining Eq. (3) leads to selecting: $t_p = m_p U/F$. The equations of motion can now be written in dimensionless form as follows (dimensionless variables have a tilde) :

$$\mathrm{Re_p}\left(\frac{\partial \tilde{\mathbf{u}}_f}{\partial \tilde{t}} + \tilde{\mathbf{u}}_f \cdot \nabla \tilde{\mathbf{u}}_f\right) = -\frac{P\rho_f a}{\mu U}\nabla \tilde{p} + \Delta \tilde{\mathbf{u}}_f \tag{4}$$

where P is the pressure scale [here $P = \mu U/(\rho_f a)$] and $\mathrm{Re_p} = \rho_f U a/\mu$ is the particle Reynolds number. For the particle, one obtains:

$$\mathrm{St}\frac{d\tilde{\mathbf{u}}_p}{d\tilde{t}} = \frac{m_p}{F}\mathbf{g} + \tilde{\mathbf{F}}(\tilde{\mathbf{u}}_p, \tilde{\mathbf{u}}_f) \tag{5}$$

where $\mathrm{St} = t_p/t_f$ is called the Stokes number. Two asymptotic regimes can be achieved depending on the value of the Stokes number:

- $\mathrm{St} \gg 1$. The fluid has no time to adjust its velocity to the variations in the particle velocity and, conversely, the particle is not affected by the rapid variations in the fluid velocity (but naturally it continues to be affected by the slow variations). In practice, this means that the fluid and the particle evolve in a quasi-autonomous way and, therefore, their motion can be considered separately. On a macroscopic scale, such suspensions retain a genuinely two-phase character and the equations of motion take the form of two interrelated equations (one for each phase).

- $\mathrm{St} \to 0$. The particle has time to adjust its velocity to any change in the fluid velocity field. As an illustration, one says that the particle is the slave of the fluid phase. On a macroscopic scale, this means that the suspension behaves as a one-phase medium.

From this discussion, one must keep in mind that, if in essence any particle suspension is a two-phase material on a particle scale, the suspension can also behave as a one-phase fluid on a macroscopic scale as. In addition the only asymptotic regimes for which it is possible to deduce the fluid-particle interaction in a completely theoretical way are the regimes $\mathrm{St} \to 0$ and $\mathrm{Re_p} \to 0$ and $\mathrm{St} \to \infty$ and $\mathrm{Re_p} \to \infty$. More information can be found in the review papers by Buyevich & Shchelchkova (1978), Herczynski & Pienkowska (1980), Koch & Hill (2001), the book by Kim & Karrila (1991), and the article by Ancey et al. (1999).

2.2 Bulk equations of motion

We now turn to the problem of a collection of particles in a Newtonian fluid, and more specifically, we will try to build the bulk constitutive equation from the local equations of motion (1) and (2). To this end, we consider a homogeneous suspension whose density number in particles is n [n is related to the volume solid concentration ϕ by $n = \phi/(4\pi a^3/3)$]. The basic idea is to average the local equations to obtain mean equations. To do this, we use a "volume averaging" process, which involves taking the volume average (over a sufficiently large volume $\mathcal{V}$) of any quantity $f(\mathbf{x}, t)$:

$$\bar{f}(\mathbf{x}, t) = \frac{1}{\mathcal{V}} \int_{\mathcal{V}} f(\mathbf{x}, t) d\mathcal{V} \tag{6}$$

Since we integrate fields that are defined only on either phase while the integration volume $\mathcal{V}$ includes both phases indistinctly, we define a characteristic function H, which is zero in fluid and unity in particle. By definition, we have: $\bar{H} = \phi$. Multiplying the equation of motion (1) by $1 - H$, then integrating, using basic relationships (e.g., $\nabla H = \mathbf{k}$), and after algebraic manipulations, we find that the averaged equation of motion for the fluid phase is:

$$\rho_f \left(\frac{\partial \overline{\mathbf{u}}_f}{\partial t} + \nabla \cdot \overline{\mathbf{u}}_f \overline{\mathbf{u}}_f \right) = -\nabla \bar{p} + \frac{1}{\mathcal{V}} \int_{\mathcal{A}_p} (\sigma_f - p\mathbf{1}) \cdot \mathbf{k} d\mathcal{A} + \nabla \cdot \frac{1}{\mathcal{V}} \int_{\mathcal{V}_f} (\sigma_f - \rho_f \mathbf{u'}_f \mathbf{u'}_f) d\mathcal{V} \tag{7}$$

where $\mathcal{V}_f$ (resp. $\mathcal{V}_p$) is the sub-volume of $\mathcal{V}$ including the fluid phase (resp. particle phase); $\mathcal{A}_p$ is the frontier surface surrounding $\mathcal{V}_p$; $\mathbf{k}$ is a vector normal to $\mathcal{A}_p$; $\mathbf{u}_f = \bar{\mathbf{u}}_f + \mathbf{u}'_f$ is the Reynolds decomposition of the fluid velocity into a mean value $\bar{\mathbf{u}}_f$ and a fluctuating term $\mathbf{u}'_f$. Similarly, for the particle phase, we obtain:

$$\rho_p \left(\frac{\partial \overline{\mathbf{u}}_p}{\partial t} + \nabla \cdot \overline{\mathbf{u}}_p \overline{\mathbf{u}}_p \right) = \phi \rho_p \mathbf{g} + \nabla \cdot (\overline{\sigma}_p - \rho_p \overline{\mathbf{u'}_p \mathbf{u'}_p}) - \frac{1}{\mathcal{V}} \int_{\mathcal{A}_p} \sigma_p \cdot \mathbf{k} d\mathcal{A} \tag{8}$$

We should note that, at the particle boundaries, we have equality of the stress state, that is: $\sigma_p \cdot \mathbf{k} = (\sigma_f - p\mathbf{1}) \cdot \mathbf{k}$. In both equations above, a term $\int_{\mathcal{A}_p} \sigma_p \cdot \mathbf{k} d\mathcal{A}$ has appeared: it represents the momentum transfer between the two phases and plays a fundamental role in the rheology of two-phase flows.

We now introduce a bulk velocity as the volume average velocity: $\overline{\mathbf{u}}(\mathbf{x}, t) = \overline{\mathbf{u}}_p(\mathbf{x}, t) + \overline{\mathbf{u}}_f(\mathbf{x}, t)$. A density average velocity can be built as well: $\bar{\rho} \overline{\mathbf{u}}_m = \rho_p \overline{\mathbf{u}}_p + \rho_f \overline{\mathbf{u}}_f$, with $\bar{\rho} = \phi \rho_p + (1 - \phi) \rho_f$. The two velocities do coincide exactly when the phase densities match ($\rho_p = \rho_f$) or approximately when one density is much larger than the other ($\rho_p \gg \rho_f$ or $\rho_p \ll \rho_f$). Adding Eqs. (7) and (8) provides the bulk equation of motion:

$$\bar{\rho} \left(\frac{\partial \overline{\mathbf{u}}_m}{\partial t} + \nabla \cdot \overline{\mathbf{u}}_m \overline{\mathbf{u}} \right) = -\nabla \bar{p}^\star + \nabla \cdot \frac{1}{\mathcal{V}} \int_{\mathcal{V}} (\sigma - (\rho \mathbf{u})' \mathbf{u}') d\mathcal{V} \tag{9}$$

where $\bar{p}^\star = \bar{\Phi} + \bar{p}_f$ (with $\nabla \bar{\Phi} = -\bar{\rho} \mathbf{g}$). This form is very interesting provided it takes the classic form of a momentum balance in a continuum, that is, only when $\overline{\mathbf{u}}_m \approx \overline{\mathbf{u}}$ so that the

terms in the right-hand side can be approximated by a material derivative. If so, the bulk stress tensor is then:

$$\bar{\sigma} = \frac{1}{\mathcal{V}} \int_{\mathcal{V}} (\sigma - \rho \mathbf{u}'\mathbf{u}') d\mathcal{V} \tag{10}$$

which is nothing more than the definition of the bulk stress given by Batchelor (1974). By construction, this tensor can be broken into a fluid contribution and a particle contribution. The latter takes the form (Ancey et al. 1999):

$$\bar{\sigma}^{(p)} = \frac{1}{\mathcal{V}} \int_{\mathcal{A}_p} \sigma \cdot \mathbf{x}\mathbf{k} d\mathcal{A} - \frac{1}{\mathcal{V}} \int_{\mathcal{V}_p} \rho_p \mathbf{u}'\mathbf{u}' d\mathcal{V} + \mathbf{G}(\omega_p) \tag{11}$$

where $\mathbf{G}(\omega_p)$ is an antisymmetric function of the particle rotational velocity ω_p ($\mathbf{G}$ vanishes in most cases of interest). The second term in the right-hand side of Eq. (11) represents the stress due to the flux of fluctuating momentum, a key ingredient in kinetic theory. The first term represents the bulk stress generated by particle interactions. An alternative expression of this term can be achieved by replacing volume average by ensemble average. In doing so, one obtains: $na < \mathbf{f}\mathbf{k} >$, in which the brackets stand for the ensemble average and $\mathbf{f} = \sigma_p \cdot \mathbf{k} d\mathcal{A} = (\sigma_f - \mathbf{1}) \cdot \mathbf{k} d\mathcal{A} + \mathbf{f}_c$ is the total force acting on the particle boundary ($\mathbf{f}_c$ is the contact force exerted by a near particle).

2.3 Diagram of flow regimes

The treatment presented here has the great advantage of providing a comprehensive framework for describing (and understanding) the bulk behavior of particle suspensions. The results are consistent with those used in kinetic theories of granular materials (Reynolds stress tensor), soil mechanics (Terzaghi's principle, bulk stress in granular materials), and two-phase flow theories [for more information, see the papers by Campbell (1990), and Marchioro et al. (1999), and the book by Cambou (1998)]. To complete this framework, how to compute the different terms in the bulk stress tensor equation must be specified [Eqs. (10–11)]. There is no general theory for this purpose. Rigorous analytical results have been obtained only for certain flow conditions (e.g. when $\mathrm{Re_p}$ and St are much less than unity). To progress in determining the rheological properties of particle suspensions, the basic idea is to look for prevailing terms in Eqs. (10–11) according to the flow conditions. This is done typically by dimensional analysis. For an interaction to be predominant, it must have (i) a sufficient strength relative to others and (ii) time for its effects to influence the system. In practice, most of the dimensionless numbers we use can be interpreted in this way. For instance, the Stokes number can be seen as the ratio of particle/fluid relaxation times or the ratio of inertia/viscous effects. Using a limited number of dimensionless numbers makes it possible to outline the flow regimes in a single diagram $(\dot{\gamma}, \phi)$ where $\dot{\gamma}$ is the shear rate (see. Fig. 1) as suggested by Coussot & Ancey (1999). At low and moderate solid concentrations, most of these regimes are well identified and there is an abundant literature that can be consulted (see the review papers given in the references).

Lagging behind, the study of very concentrated suspensions dates back to the pioneering work of Bagnold. Though today challenged in his theoretical and experimental developments [see the paper by Hunt et al. (2002)], Bagnold's work contains, however, important elements

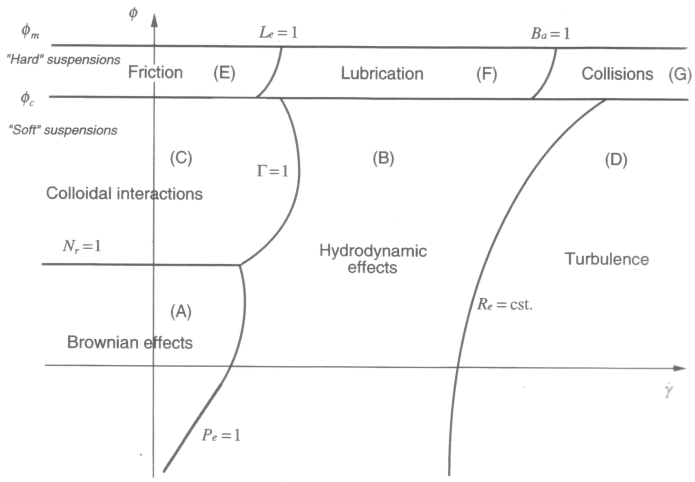

Figure 1: Simplified diagram of flow regimes. The transitions between regimes are described using dimensionless numbers: The Péclet Pe $= 6\pi\mu a^3\dot{\gamma}/(kT)$ (T the temperature, k la Boltzmann constant) for the transition between Brownian (thermal agitation of particles) and viscous regimes; the repulsion number Nr $= \Psi/(kT)$ (with Ψ the van der Waals interaction potential) for the transition between the colloidal and Brownian regimes; $\Gamma = 6\pi\mu a^3\dot{\gamma}/\Psi$ is a number reflecting the ratio between viscous and colloidal interactions; the particle or flow Reynolds number is used for the transition towards turbulence; the Leighton number Le $= \mu\dot{\gamma}a/(\epsilon\sigma_n)$ (with ϵa the mean distance between the surfaces of two close particles) for the transition between the viscous and frictional regimes; the Bagnold number Ba $= \rho_p\dot{\gamma}\epsilon a/\mu$ is used for the transition between the viscous and collisional regimes. ϕ_m denotes the maximum random solid concentration ($\phi_m \approx 0.635$ for spherical particles of equal size) and ϕ_c is the minimum concentration for a network of particles in close contact to form ($\phi_c \approx 0.5$ for spherical particles of equal size).

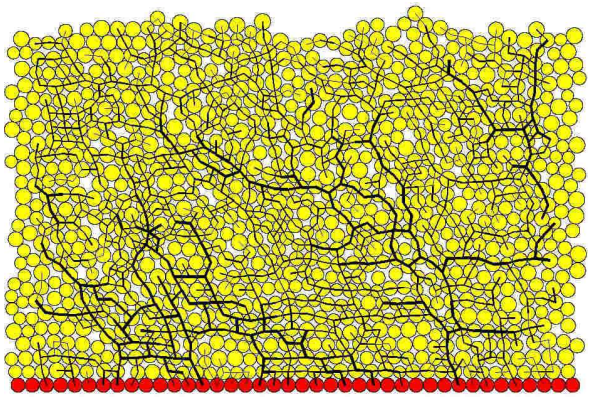

Figure 2: Simulation of force network within a granular flow. Lines represent the normal forces transmitted by the network of particles (cylinder of various size); the line thickness is related to the force strength. The channel slope is $18°$. Courtesy of M. Prochnow and F. Chevoir.

for understanding concentrated suspensions and has been the springboard for subsequent theories on granular suspensions, notably kinetic theories. At approximately the same time, a French engineer, Dantu, used photoelastic PVC cylinders to demonstrate that in granular assemblies, contact forces were transmitted through a network of particles in close contact. The formation of such a network of particles in contact (here contact is taken very broadly) has important implications in terms of bulk rheological behavior and may be associated with a number of striking phenomena (dilatancy, jamming, shear localization, etc.). Figure 2 shows a typical network obtained by Prochnow and Chevoir using a Contact-Dynamics numerical model. At the base of the flow, it can be seen that there is a significant increase in the normal force experienced by particles belonging to the network while, for particle clusters surrounding the percolating network, the force chains are much weaker (vault effect). This statistically heterogenous distribution of forces implies that very different types of particle interaction can occur, depending on whether the particles belong to a percolating network or not [see typical examples in the case of the frictional-collisional regime for granular flows given in the articles by Ancey & Evesque (2000) and Ancey (2002)].

Another striking property of concentrated particles is that contact is a strongly nonlinear process involving a great variety of physical phenomena (lubrication, elastoplastic deformation, etc.). For instance, two near-contact particles can be separated by a very thin film, which prevents particles from making contact(lubricated contact) or conversely from separating(stuck particles). To determine the prevailing particle interaction(s), a number of dimensionless numbers turn out to be helpful (see caption of Fig. 1). Taking the example of lubricated contact once again, we find that its effect on bulk dynamics can be evaluated by computing the so-called Leighton number Le, defined as the ratio of the lubrication force $3\pi\mu ac/(2\varepsilon)$ (where c and εa denote the relative particle velocity and the surface-to-surface distance) and the buoyant normal stress $\rho' gh$ [where $\rho' = \phi(\rho_p - \rho_f)$ and h are the buoyant density and the depth at which the particle locates with respect to the free surface]. Note that, in this definition, we use the buoyant stress (i.e., the weight of the column above the test particle minus the fluid pressure) and not the buoyant mass of the particle since it can belong to a percolating network. In the regime diagram (see Fig. 1), we consider that there are three

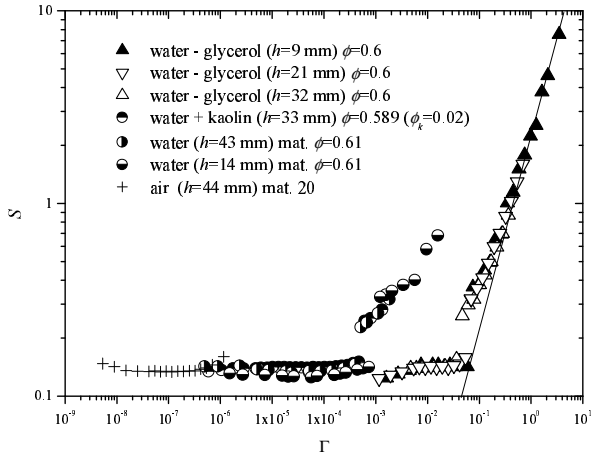

Figure 3: Variation in the dimensionless shear stress as a function of the dimensionless number Γ. The line slope is unity and indicates a linear variation of S with Γ

possible regimes depending on the predominant contact type between particles (frictional, lubricated, collisional).

2.4 Experimental evidence

In order to study the influence of lubricated contact on bulk dynamics and provide evidence of the key role played by the particle network in the rheological properties of highly concentrated suspensions, we studied a number of suspensions made up of glass beads and various interstitial fluids: air ($\mu = 1.8 \times 10^{-5}$ Pa.s), water ($\mu = 10^{-3}$ Pa.s), water-glycerol solution ($\mu = 0.96$ Pa.s, $\rho_f = 1260$ kg/m^3), and water-kaolin dispersion. The particle diameter was either 0.3 mm, 0.8 mm, 1 mm, 2 mm, or 3 mm.

Determining the rheological properties of particle suspensions is somewhat difficult due to the presence of the coarse fraction. We therefore used a vane-shear cell. This involved equipping the Haake Rotovisco MV5 rheometer with a four-blade vane centered around a vertical shaft. The blade was 30 mm in radius (R_1) and 60 mm in height. The cell was 55 mm in radius (R_2) and 90 mm in depth, with smooth walls. This technique from soil mechanics is now increasingly used in rheometry of suspensions [Barnes & Nguyen (2001)]. More information on the experimental procedure and results can be found in the papers by Ancey & Jorrot (2001a) and Ancey (2001b).

Figure 3 shows the variation of the dimensionless shear stress $S = \tau/(\rho g h)$ (where τ denotes the shear stress and h is the thickness of material sheared by the vane) as a function of a dimensionless number $\Gamma = \mu\Omega/(\rho' g h)$ (where Ω is the rotational speed of the vane), akin to a dimensionless shear rate (we replace the shear rate by the rotational speed because determining the actual shear rate for a large-gap rheometer and a material with varying rheological properties is very delicate). Let us note that this number is very close to the Leighton number introduced above (if we take $c = \mathcal{O}(\Omega a)$). Though the experimental curve reported in Fig. 3 does not provide the proper flow curve (i.e., the $\tau - \dot{\gamma}$ relationship) it can provide an approximate idea of this flow curve.

At low shear velocities ($\Gamma \ll 1$), shear was localized within a narrow cylindrical band

around the vane, with a typical thickness of approximately 10 bead diameters independently of Γ. We found that S is independent of Γ which implies, when we return to dimensional variables, that: (i) $\tau \propto \sigma_{zz}$ (where σ_{zz} denotes the vertical normal stress) and (ii) τ does not depend on the shear rate. These are two features of the frictional regime.

At high rotational speed, all the material was sheared in the gap. We observed that $S \propto \Gamma$, that is, in terms of dimensional variables, $\tau \propto \dot{\gamma}$. The bulk behavior is similar to a Newtonian fluid for these flow conditions.

A striking result of this experiment is that it is possible to observe very different bulk rheological behavior by merely increasing the shear rate and keeping the solid concentration fairly constant.

3 BIMODAL SUSPENSIONS

Natural suspensions usually involve broad particle-size distributions and particles of different chemical compositions. Thus, the approximation of equal-size particle suspension is most often useless. A first step in modeling polydisperse suspensions is to consider as many size grades as there are different types of particle interaction. However, there are many different types of particle interaction depending on the particle size, shear rate, solid concentration, ion concentration, and temperature: Brownian effects, colloidal surface forces (electrostatic attractive forces and van der Waals attractive forces), viscous forces, and contact forces (lubrication, solid friction, collision). Therefore, in the general case, determining the chief interactions within a suspension with a wide size distribution is difficult. Here we examine a limiting case of very concentrated suspensions with a bimodal size distribution, which is much easier to understand. The fine fraction is made up of colloidal particles whereas the coarse fraction includes large non-colloidal non-Brownian particles. As shown by Sengun and Probstein (1989 a,b), when the concentration in coarse particles is low to moderate, it is still possible to return to the equal-size particle suspension approximation. For very concentrated suspensions of coarse particles, interactions between particles are generally the key process in bulk stress generation and I will provide some experimental evidence for the diversity in the rheological properties of these materials.

3.1 An overview of moderately concentrated suspensions

Sengun and Probstein (1989a) have suggested that it is possible to consider polydisperse suspensions made up of fine (colloidal) and coarse (noncolloidal) particles as bimodal suspensions. Their explanation consists of two approximations. First, as it is the interstitial phase, the dispersion resulting from the mixing of fine colloidal particles and water imparts most of its rheological properties to the entire suspension. Secondly, the coarse fraction is assumed to act independently of the fine fraction and to enhance the bulk viscosity. They introduced a *net viscosity* μ_{nr} of a bimodal slurry as the product of the fine relative viscosity μ_{fr} and the coarse relative viscosity μ_{cr}. The fine relative viscosity is defined as the ratio of the apparent viscosity of the fine-particle suspension to the viscosity of the interstitial fluid: $\mu_{fr} = \mu_f/\mu_0$. The coarse relative viscosity is defined as the ratio of the apparent viscosity of the coarse-particle slurry to the viscosity of the fine-particle suspension: $\mu_{cr} = \mu_c/\mu_f$. The two relative viscosities depend on the solid concentrations and a series of generalized

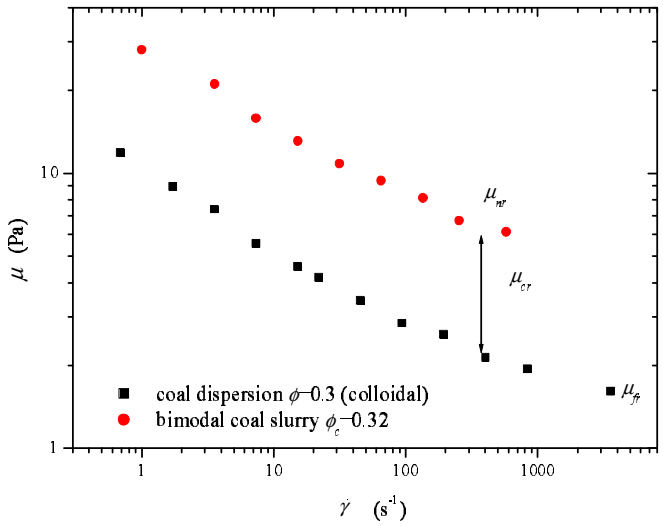

Figure 4: Variation of the bulk viscosity of coal slurry as a function of the shear rate. The bulk viscosity curve is parallel to the curve obtained with the fine fraction. After Sengun and Probstein (1989b).

Péclet numbers. For the coarse-particle suspensions, all the generalized Péclet numbers are much greater than unity. Using a dimensional analysis, Sengun and Probstein deduced that the coarse relative viscosity cannot depend on the shear rate. In contrast, bulk behavior in fine-particle suspensions is governed by colloidal particles and thus at least one of the generalized Péclet numbers is of the order of unity, implying that the fine relative viscosity is shear-dependent. Sengun and Probstein's (1989b) experiments on viscosity of coal slurries confirmed the reliability of this concept. Plotting $\log \mu_{nr}$ and $\log \mu_{fr}$ against $\log \dot{\gamma}$, they found that over a wide range of concentrations, the curves were parallel and their distance was equal to $\log \mu_{cr}$ (see Fig. 4). However, for solid concentrations in the coarse fraction exceeding 0.35, they observed a significant departure from parallelism, which they ascribed to nonuniformity in the shear rate distribution within the bulk due to squeezing effects between coarse particles. In this case, it may be suspected that coarse particles begin to interact.

3.2 Concentrated bimodal suspensions

A solid theoretical rheophysical analysis of bimodal suspensions (including colloidal and noncolloidal) is beyond our current capacity. The approximation proposed by Sengun and Probstein is very helpful for a fairly wide range of solid concentrations but fails at high solid concentrations in coarse particles, as I will show through two typical experiments.

3.2.1 Yield stress of a bimodal suspension

When added to water, kaolin particles form a viscoplastic dispersion. Yield stress is directly connected with the solid concentration in kaolin ϕ_k. For instance, Zhou et al. (1999) have shown that:

$$\tau_c \propto (\phi_k/(1-\phi_k))^c \tag{12}$$

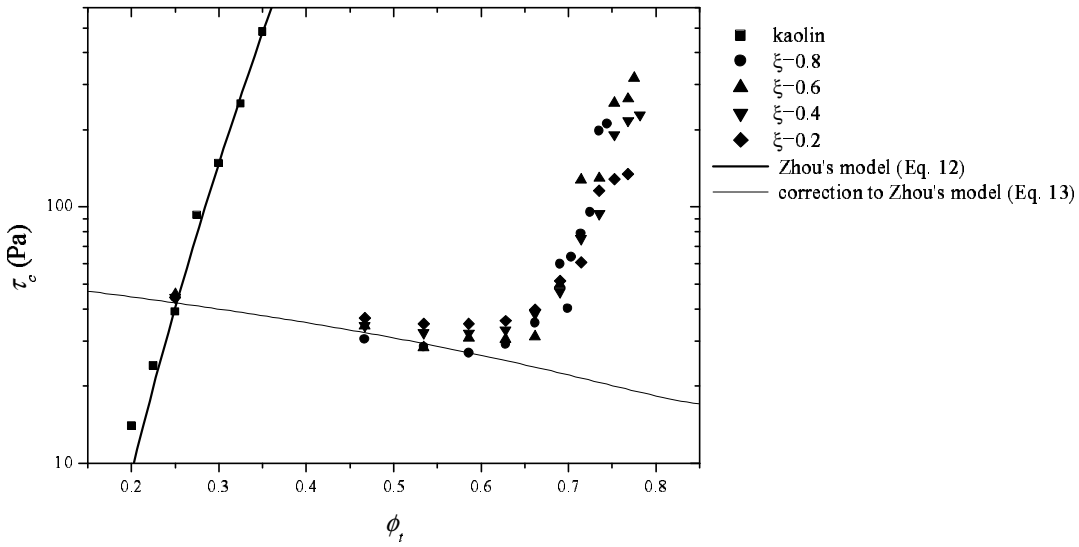

Figure 5: Variation of the bulk yield stress.

The question is: what happens when coarse particles are added to this dispersion. At first glance, since the volume occupied by the colloidal particles is decreased, the bulk yield stress should decrease and, to first order, we should have:

$$\tau \propto (\phi_k/(1-\phi_k))^c (1-\phi_c) \tag{13}$$

where ϕ_c is the coarse-particle concentration. To test this expectation, I measured the bulk yield stress of kaolin suspensions to which I added a given amount of coarse particles. Due to the large size of coarse particles used (typically 1 mm in diameter) relative to the gap size of conventional rheometers, I used the slump test method as described by Pashias et al. (1996). In order to test the influence of size distribution of coarse particles and particle roundness, equal-size glass beads, bimodal mixtures of glass beads, and sand were used as coarse particles.

Figure 5 shows typical results obtained with a bimodal distribution of glass beads (1 mm and 3 mm in diameter). The dimensionless number ξ is the relative fraction of small beads ($\xi = 0$ means that there were no small beads while $\xi = 1$ means that all coarse particles added to the kaolin suspension were small beads). The total solid concentration ϕ_t is computed as follows: $\phi_t = \phi_k(1-\phi_c) + \phi_c$. The first result is that the trend given by Eq. (13) is correct to first order: adding a small amount of coarse particles leads to a decrease in the bulk yield stress (here for total solid concentrations as high as 0.55). Interestingly enough, in contrast with our previous expectation, the bulk yield stress starts blowing up when the total solid concentration comes closer to the maximum solid concentration. A striking feature of this abrupt rise is that the increase rate is very close to the value measured for a pure kaolin dispersion. This could mean that all happens as if coarse particles surrounded by colloidal particles behaved in turn as colloidal particles (this statement is naturally wrong). Further comments on Fig. 5 are the following:

- At low and moderate concentrations in coarse particles, the bulk yield stress was independent of the particle size (when equal size distributions were tested) but it increases

significantly with increasing relative fractions of large particles.

- On the contrary, at high concentration, the finer the distribution, the larger the yield stress.

The main and unexpected result of this experimental study is that bulk yield stress may be significantly affected by the concentration of coarse particle but its features (such as the growth rate with solid concentration) are still ruled by the fine colloidal fraction.

3.2.2 Flow curve of a bimodal suspension

After studying yielding conditions, dynamic conditions will be examined. We return to the experiment described in Sec. 2.4. The cell was poured with a suspension of glass beads in water; the solid concentration ϕ_c was very close to the maximum concentration ϕ_m (here we have $\phi_c = 0.6$ while $\phi_m = 0.635$). Kaolin particles were added to the suspension. The question is: in which way is bulk behavior affected by adding these particles? Experimental data are reported in Fig. 6, showing the torque exerted by the suspension on the vane as a function of its dimensionless rotational speed Γ. Obviously, when the solid concentration in kaolin ϕ_k is low, there is not much difference compared to the results found in Sec. 2.4. Conversely, when ϕ_k is sufficiently high, bulk behavior is expected to be viscoplastic (Sengun and Probstein's approximation). Both statements are right, as shown in Fig. 6 (material A refers to a suspension poor in kaolin while material C is rich in kaolin). At intermediate concentration ϕ_k (material B in Fig. 6), an odd behavior was observed. The time measurement of the torque revealed that, when a shear rate was applied, the shear stress first increased rapidly and reached a maximum (short-term behavior), then decreased slowly and flattened out, and rose once again to finally attain its late-time value (typically after 1000 revolutions of the vane). Reporting the early-time and late-time values of the measured torque in Fig. 6, we observed a complicated response of the material: over a short time span, it behaved like a power-law (shear-thinning) fluid while, over a long time span, its flow curve was identical to that of material A. A possible explanation of this behavior is that, when a shear rate step is applied, the network of particles is broken and contact between coarse particles is lubricated by the kaolin-water suspension. Since the yield stress of the kaolin-water suspension is not sufficient for coarse particle sedimentation to be hindered, a network of particles in close contact forms again after a finite time.

This experiment illustrates the diversity observed in debris flow behavior. In this respect, material A is typical of materials involved in granular debris flows while material C represents the class of muddy debris flows. Between these two classes, material B could be representative of lahar-like flows. A striking result is that small changes in the relative fraction can lead to profound modifications in the structure of the constitutive equation.

4 CONCLUDING REMARKS

This paper has reviewed a number of important concepts used in the rheophysical approach to particle suspensions and provided a number of connections between theoretical analysis, laboratory experiments on simple particle suspensions, and debris flows. For highly concentrated suspensions, bulk behavior depends a great deal on the formation of force chains

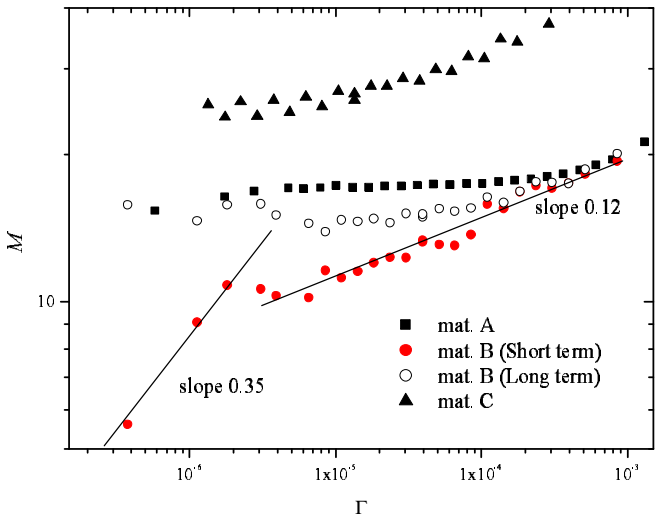

Figure 6: Variation of the dimensionless torque $M = C/(\pi\rho' ghR_1^3)$ (where C is the measured torque) exerted on the vane by the tested suspension as a function of the rotational speed Γ. Material A: $\phi_k = 3.2\%$, $\phi_c = 60.6\%$, $\phi_t = 61.8\%$. Material B: $\phi_k = 9.8\%$, $\phi_c = 58.9\%$, $\phi_t = 62.9\%$. Material C: $\phi_k = 15.4\%$, $\phi_c = 47.9\%$, $\phi_t = 55.9\%$.

between the coarsest particles (particle network). Depending on whether contact between coarse particles is lubricated by the mixture made up of water and fine particles (matrix), the rheological properties may vary significantly: power-law, viscoplastic, frictional, etc. In this respect, laboratory experiments successfully represent the diversity in the rheological behavior of real debris flows such as those described in the literature [see the review by Coussot (1997) and Iverson (1997)]. They have also shown complex time-dependent responses of suspensions for certain size distributions, a result in line with measurements made by Contreras & Davies (2000) on samples collected from debris flow deposits.

ACKNOWLEDGEMENTS

Through PNRN (Programme National sur les Risques Naturels), the Institut National des Sciences de l'Univers (INSU) is thanked for its continued support.

REFERENCES

Ancey, C., Coussot, P. & Evesque, P. 1999. A theoretical framework for very concentrated granular suspensions in a steady simple shear flow. *Journal of Rheology* 43: 673–1699.

Ancey, C. & Evesque, P. 2000. Frictional-collisional regime for granular suspension flows down an inclined channel. *Physical Review E* 65: 8349–8360.

Ancey, C. & Jorrot, H. 2001. Yield stress for particle suspensions within a clay dispersion. *Journal of Rheology* 45: 297–319.

Ancey, C. 2001. Role of lubricated contacts in concentrated polydisperse suspensions. *Journal of Rheology* 45: 1421–1439.

Ancey, C. 2002. Dry granular flow down an inclined channel: Experimental investigations on the frictional-collisional regime. *Physical Review E 65*: 11304.

Barnes, H.A. & Nguyen, Q.D. 2001. Rotating vane rheometry – A review. *Journal of Non-Newtonian Fluid Mechanics* 98: 1–14.

Batchelor, G.K. 1974. Transport properties of two-phase materials with random structure. *Annual Review of Fluid Mechanics*. 6: 227–255.

Buyevich, Y.A. & Shchelchkova, I.N. 1978. Flow of dense suspension. *Progress in Aerospace Science* 18: 121–150.

Cambou, B. 1998. *Behaviour of Granular Materials*. New York: Springer.

Campbell, C.S. 1990. Rapid granular flows. *Annual Review of Fluid Mechanics* 22: 57-92.

Contreras, S.M. & Davies, T.R.H. 2000. Coarse-grained debris-flows: hysteresis and time-dependent rheology. *Journal of Hydraulic Engineering* 126: 938–941.

Coussot, P. 1997. *Mudflow Rheology and Dynamics*. Rotterdam: Balkema.

Coussot, P. & Ancey, C. 1999. Rheophysical classification of concentrated suspensions and granular pastes. *Physical Review E*. 59: 4445–4457.

Herczynski, R. & Pienkowska, I. 1980. Toward a statistical theory of suspension. *Annual Review of Fluid Mechanics* 12:237–269.

Hunt, M.L., Zenit, R., Campbell, C.S. & Brennen, C.E. 2002. Revisiting the 1954 suspension experiments of R. A. Bagnold. *Journal of Fluid Mechanics* 452: 1–24.

Iverson, R.M. 1997. The physics of debris flows. *Review of Geophysics* 35: 245–296.

Kim, S. & Karrila, S.J. 1991. *Microhydrodynamics: Principles and Selected Applications*. Stoneham: Butterworth-Heinemann.

Koch, D.L. & Hill, R.J. 2001. Inertial effects in suspension and porous-media flows. *Annual Review of Fluid Mechanics* 33: 619–647.

Marchioro, M., Tanksley, M. & Prosperetti, A. 1999. Mixture pressure and stress in disperse two-phase flow. *International Journal of Multiphase Flow* 25: 1395–1429.

Pashias, N. & Boger, D.V. 1996. A fifty cent rheometer for yield stress measurement. *Journal of Rheology* 40:1179-1189.

Sengun, M.Z. & Probstein, R.F. 1989a. Bimodal model of slurry viscosity with applications to coal slurries. Part 1. Theory and experiment. *Rheologica Acta* 28: 382–393.

Sengun, M.Z. & Probstein, R.F. 1989b. Bimodal model of slurry viscosity with applications to coal slurries. Part 2. High shear limit behaviour. *Rheologica Acta* 28: 394–401.

Zhou, Z., M.J. Solomon, Scales, P.J. & Boger, D.V. 1999. The yield stress of concentrated flocculated suspensions of size distributed particles. *Journal of Rheology* 43: 651–671.